Notes

NMR Shifts, Orbitals, and M···H−X Bonding in d^8 Square Planar Metal Complexes

Yong Zhang,[†] Jared C. Lewis,[‡] Robert G. Bergman,[‡] Jonathan A. Ellman,[‡] and Eric Oldfield*,[†]

Department of Chemistry, University of Illinois at Urbana−Champaign, 600 South Mathews Avenue, Urbana, Illinois 61801, and Department of Chemistry, University of California, Berkeley, California 94702

Received February 20, 2006

Summary: We have investigated M···H−C interactions in d^8 square planar Rh and Pt complexes involving different types of C−H bonds, as well as a M···H−N hydrogen-bonded complex, using a combination of DFT and "atoms-in-molecules" (AIM) theory. The AIM analysis shows that both M···H−C and M···H−N interactions in d^8 square planar complexes are of a closed-shell, electrostatic nature, similar to protein backbone hydrogen bonds. However, at the shortest M···H distances, both interactions have partial covalence. We find no evidence for the involvement of d_{z^2} orbitals in M···H−C interactions but do find evidence for the involvement of $d_{xz/yz}$ orbitals in M···H−C bonding. The DFT calculations reproduce well the experimental proton NMR chemical shifts, with a theory-versus-experiment correlation coefficient $R^2 = 0.985$. There are large downfield ^{1}H NMR chemical shift changes on metal bonding, accompanied by changes in shielding tensor orientations.

The activation of X−H bonds by transition metals is a topic of broad general interest and importance,[1−5] and a number of reports have indicated the involvement of X−H···M interactions along the reaction coordinate for X−H activation by transition metal species.[6−8] In contrast to d^6 complexes having agostic interactions (I) with small M−H bond lengths (ca. 1.8−2.3 Å) and M−H−C angles (ca. 90−140°), both the M···H−C interactions (II) and M···H−N interactions (III) in d^8 square planar complexes have relatively large M···H distances (ca. 2.3−2.9 Å in II and 2.1−2.8 Å in III) as well as M−H−X angles (ca. 110−170° in II and 140−170° in III).[5]

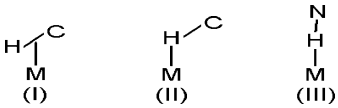

Moreover, while agostic complexes (I) are characterized by upfield (more shielded) ^{1}H NMR chemical shifts compared to their free ligands, both M···H−C (II) and M···H−N (III) complexes have more downfield (or deshielded) ^{1}H NMR shifts,[5] a general feature of hydrogen bonds (HBs).[9] However, while the M···H−N interaction (III) has been generally accepted as a hydrogen bond, the nature of the M···H−C interaction (II) in d^8 square planar complexes, the nature of preagostic (or pregostic)[2a,10] interactions, is still a topic of debate,[3,5] and it was therefore recently proposed[3] that appropriate high-level theoretical calculations be carried out to shed light on this situation.

Here, we present the results of such a quantum chemical analysis of the ^{1}H NMR chemical shifts and bonding in several different preagostic complexes (II): [Rh(cyclo-octa-1,5-diene)(Fe{η^5-C_5H_4(2-C_5H_4N)}η^5-$C_5H_4PPh_2$)]PF_6 (**1**), containing an aromatic (ferrocene) C−H···M interaction;[11] *trans*-$PtCl_2$(quinoline-8-carbaldehyde)PEt_3 (**2**), containing an aldehyde C−H···M interaction;[12] and [RhCl(*i*-Pr_2POXy)(PMe_3)]$_2$ (Xy = 2,3-xylyl, **3**), containing a phenyl C−H···M interaction.[7] We also investigated one HB complex, *cis*-[Pt(*o*-$Ph_2PC_6H_4NC(O)C_6H_4$][*o*-$Ph_2PC_6H_4NHC(O)Ph$)] (**4**),[13] for comparison. The structures of these systems are shown in Figure 1 and cover a variety of M···H interactions in d^8 square planar complexes, spanning essentially the entire experimental range in M···H distances (2.3−3.0 Å).[5,7,11−13] The M···H bonding in these preagostic and HB metal complexes was studied in a quantitative manner by using an atoms-in-molecules (AIM) theory approach,[14] as employed previously in investigating hydrogen bonding in proteins[15] and other systems.[4,9]

We first calculated the ^{1}H NMR chemical shifts using a locally dense basis set scheme with the B3LYP functional,[16,17]

* To whom correspondence should be addressed. E-mail: eo@chad.scs.uiuc.edu.

† University of Illinois at Urbana−Champaign.

‡ University of California, Berkeley.

(1) Zhao, J.; Goldman, A. S.; Hartwig, J. F. *Science* **2005**, *307*, 1080.

(2) (a) Krumper, J. R.; Gerisch, M.; Magistrato, A.; Rothlisberger, U.; Bergman, R. G.; Tilley, T. D. *J. Am. Chem. Soc.* **2004**, *126*, 12492. (b) Stepien, M.; Latos-Grazynski, L.; Szterenberg, L.; Panek, J.; Latajka, Z. *J. Am. Chem. Soc.* **2004**, *126*, 4566.

(3) Brammer, L. *Dalton Trans.* **2003**, 3145.

(4) Popelier, P. L. A.; Logothetis, G. *J. Organomet. Chem.* **1998**, *555*, 101.

(5) Wenbin, Y.; Eisenstein, O.; Crabtree, R. H. *Inorg. Chim. Acta* **1997**, *254*, 105.

(6) Davies, D. L.; Donald, S. M. A.; Macgregor, S. A. *J. Am. Chem. Soc.* **2005**, *127*, 13754.

(7) Lewis, J. C.; Wu, J.; Bergman, R. G.; Ellman, J. A. *Organometallics* **2005**, *24*, 5737.

(8) Hall, C.; Perutz, R. N. *Chem. Rev.* **1996**, *96*, 3125.

(9) Steiner, T. *Angew. Chem., Int. Ed.* **2002**, *41*, 48.

(10) (a) Crabtree, R. H. *Angew. Chem., Int. Ed. Engl.* **1993**, *32*, 789. (b) Bortolin, M.; Bucher, U.; Reugger, H.; Venanzi, L. M.; Albinati, A.; Lianza, F. *Organometallics* **1992**, *11*, 2514. (c) Cano, M.; Heras, J. V.; Maeso, M.; Alvaro, M.; Fernndez, R.; Pinilla, E.; Campo, J. A.; Monge, A. *J. Organomet. Chem.* **1997**, *534*, 159.

(11) Yoshida, T.; Tani, K.; Yamagata, T.; Tatsuno, Y.; Saito, T. *Chem. Commun.* **1990**, 292.

(12) Albinati, A.; Arz, C.; Pregosin, P. *Inorg. Chem.* **1987**, *26*, 503.

(13) Hedden, D.; Roundhill, D. M.; Fultz, W. C.; Rheingold, A. L. *Organometallics* **1986**, *5*, 336.

(14) Bader, R. F. W. *Atoms in Molecules−a Quantum Theory*; Oxford University Press: Oxford, 1990. Bader, R. W. F. *J. Phys. Chem. A* **1998**, *102*, 7314. Biegler-Knig, F. *AIM2000*, Version 1.0; University of Applied Science: Bielefeld, Germany.

10.1021/om060163h CCC: $33.50 © 2006 American Chemical Society
Publication on Web 06/10/2006

Table 1. M···H Distances ($d_{M\cdots H}$),[1]H NMR Chemical Shifts (δ), [1]H Chemical Shift Changes ($\Delta\delta$) Due to Complex Formation, and Bond Critical Point (BCP) Properties for M···H Interactions in 1−4

system	1	2	3	4	HB[e]	agostic[f]
$d_{M\cdots H}^{expt}$ (Å)[g]	2.39(5)[a]	2.6(1)[b]	3.01(4)[c]	2.318(22)[d]		
$d_{M\cdots H}^{calc}$ (Å)	2.35	2.51	2.80	2.37		
δ^{expt} (ppm)	7.82[a]	13.09[b]	9.51[c]	11.0[d]		
δ^{calc} (ppm)	8.23	13.68	9.68	12.01		
$\Delta\delta^{expt}$ (ppm)	3.09[a]	1.61[b]	2.40[c]	2.3[d]	downfield	upfield
$\Delta\delta^{calc}$ (ppm)	2.83	1.58	2.23	1.88		
$\rho(\mathbf{r})$ (au)	0.024	0.023	0.012	0.025	0.012−0.025	0.04−0.05
$G(\mathbf{r})$ (au)	0.018	0.017	0.007	0.016	0.004−0.026	
$-V(\mathbf{r})$ (au)	0.019	0.016	0.007	0.016	0.003−0.024	
$\nabla^2\rho(\mathbf{r})$ (au)	0.067	0.072	0.031	0.059	0.020−0.109	0.15−0.25
$H(\mathbf{r})$ (au)	−0.001	0.001	0.001	−0.001	0.001−0.003	

[a] Reference 11. [b] Reference 12. [c] Reference 7. $d_{M\cdots H}$ is an average in the dimer. [d] Reference 13. [e] Reference 15. BCP ranges of protein backbone HBs. [f] Reference 4. BCP ranges of some agostic complexes. [g] The M···H hydrogen atoms in complexes **1**, **2**, and **4** were located during the refinement processes used in each case. The hydrogen atom in **3** was included (idealized d_{C-H} of 0.95 Å) but not refined.

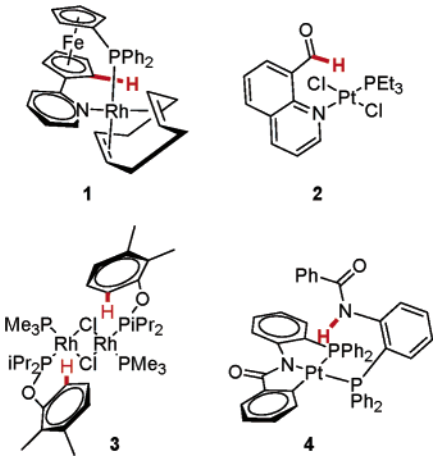

Figure 1. Molecular structures of complexes studied (the protons of interest are shown in red).

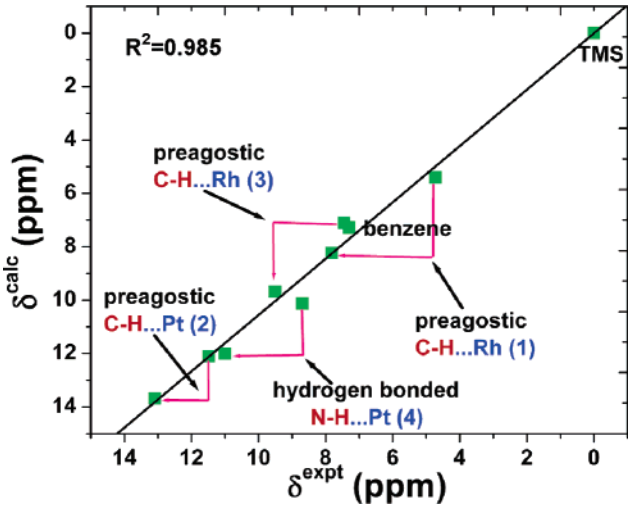

Figure 2. Plot of computed versus experimental [1]H NMR chemical shifts (pink lines connect shifts of the protons involved in M···H−X interactions, in the complex and in the free ligand).

basically the same approach used previously to evaluate the NMR properties of other metal complexes.[18] A 6-311++G-(2d,2p) basis was used for the protons of interest and their neighboring atoms, while metals were described by the SDD basis[19a] and 6-31G* and 3-21G* were used for other nonmetal atoms (see Experimental Section for details). Geometry optimization was performed using the mPW1PW91/SDD method[19a,b] (see Tables S1−S4 for optimized coordinates), as used previously with other Pt complexes.[20] X-ray crystal structures of **1** minus its PF_6^- counterion, **2**, **3** (modeled by $[RhCl(PMe_3)(Me_2POXy)]_2$), and **4** were used as starting geometries and contained 73, 44, 84, and 95 atoms, respectively. As shown by the experimental and optimized $d_{M\cdots H}$ values in Table 1, the basic geometries of the M···H−X interactions (II, III) were retained in the optimized structures and there were only small bond length/bond angle changes.

As can be seen in Table 1 and Figure 2, the computed [1]H NMR chemical shifts (referenced to TMS) of all preagostic complexes (**1**−**3**), as well as the hydrogen-bonded species (**4**), are in excellent accord with experiment, as is the chemical shift of benzene (7.28 ppm, versus 7.3 ppm from experiment[21]), included as a reference. On average, the difference between theory and experiment is 0.55 ppm for the four metal complexes, which cover a 5.3 ppm experimental shift range. Moreover, the predicted free ligand shifts in **1**−**4** of 5.40, 12.10, 7.45, and 10.13 ppm are also in good accord with experiment: 4.73, 11.48, 7.11, and 8.7 ppm. The overall prediction performance in Figure 2 has an $R^2 = 0.985$, a slope = 1.06, and an intercept = 0.01 ppm with an rms error = 0.49 ppm. The downfield [1]H NMR chemical shift changes ($\Delta\delta$) seen experimentally in both type II and III complexes are also well reproduced, as shown in Table 1. In addition, the shielding tensor results (Table 2) show that there is a 1.60 ± 0.55-fold increase in the span of the [1]H shielding tensors on complex formation, indicating major changes due to M···H interactions, with σ_{11} and σ_{22} dominating the isotropic shielding trends, Figure S1. As may be seen in

(15) Arnold, W. D.; Oldfield, E. *J. Am. Chem. Soc.* **2000**, *122*, 12835.
(16) Becke, A. D. *J. Chem. Phys.* **1993**, *98*, 5648.
(17) Frisch, M. J.; Trucks, G. W.; Schlegel, H. B.; Scuseria, G. E.; Robb, M. A.; Cheeseman, J. R.; Montgomery, J. A., Jr.; Vreven, T.; Kudin, K. N.; Burant, J. C.; Millam, J. M.; Iyengar, S. S.; Tomasi, J.; Barone, V.; Mennucci, B.; Cossi, M.; Scalmani, G.; Rega, N.; Petersson, G. A.; Nakatsuji, H.; Hada, M.; Ehara, M.; Toyota, K.; Fukuda, R.; Hasegawa, J.; Ishida, M.; Nakajima, T.; Honda, Y.; Kitao, O.; Nakai, H.; Klene, M.; Li, X.; Knox, J. E.; Hratchian, H. P.; Cross, J. B.; Adamo, C.; Jaramillo, J.; Gomperts, R.; Stratmann, R. E.; Yazyev, O.; Austin, A. J.; Cammi, R.; Pomelli, C.; Ochterski, J. W.; Ayala, P. Y.; Morokuma, K.; Voth, G. A.; Salvador, P.; Dannenberg, J. J.; Zakrzewski, V. G.; Dapprich, S.; Daniels, A. D.; Strain, M. C.; Farkas, O.; Malick, D. K.; Rabuck, A. D.; Raghavachari, K.; Foresman, J. B.; Ortiz, J. V.; Cui, Q.; Baboul, A. G.; Clifford, S.; Cioslowski, J.; Stefanov, B. B.; Liu, G.; Liashenko, A.; Piskorz, P.; Komaromi, I.; Martin, R. L.; Fox, D. J.; Keith, T.; Al-Laham, M. A.; Peng, C. Y.; Nanayakkara, A.; Challacombe, M.; Gill, P. M. W.; Johnson, B.; Chen, W.; Wong, M. W.; Gonzalez, C.; Pople, J. A. *Gaussian 03*; Gaussian, Inc.: Pittsburgh, PA, 2003.
(18) (a) Godbout, N.; Havlin, R.; Salzmann, R.; Debrunner, P. G.; Oldfield, E. *J. Phys. Chem. A* **1998**, *102*, 2342. (b) Zhang, Y.; Sujoy, M.; Oldfield, E. *J. Am. Chem. Soc.* **2005**, *127*, 2370.
(19) (a) Leininger, T.; Nicklass, A.; Stoll, H.; Dolg, M.; Schwerdtfeger, P. *J. Chem. Phys.* **1996**, *105*, 1052. (b) Adamo, C.; Barone, V. *J. Chem. Phys.* **1998**, *108*, 664.
(20) Zhang, Y.; Guo, Z.; You, X.-Z. *J. Am. Chem. Soc.* **2001**, *123*, 9378.
(21) Duncan, T. M. *Chemical Shift Tensors*, 2nd ed.; The Farragut Press: Madison, WI, 1997.

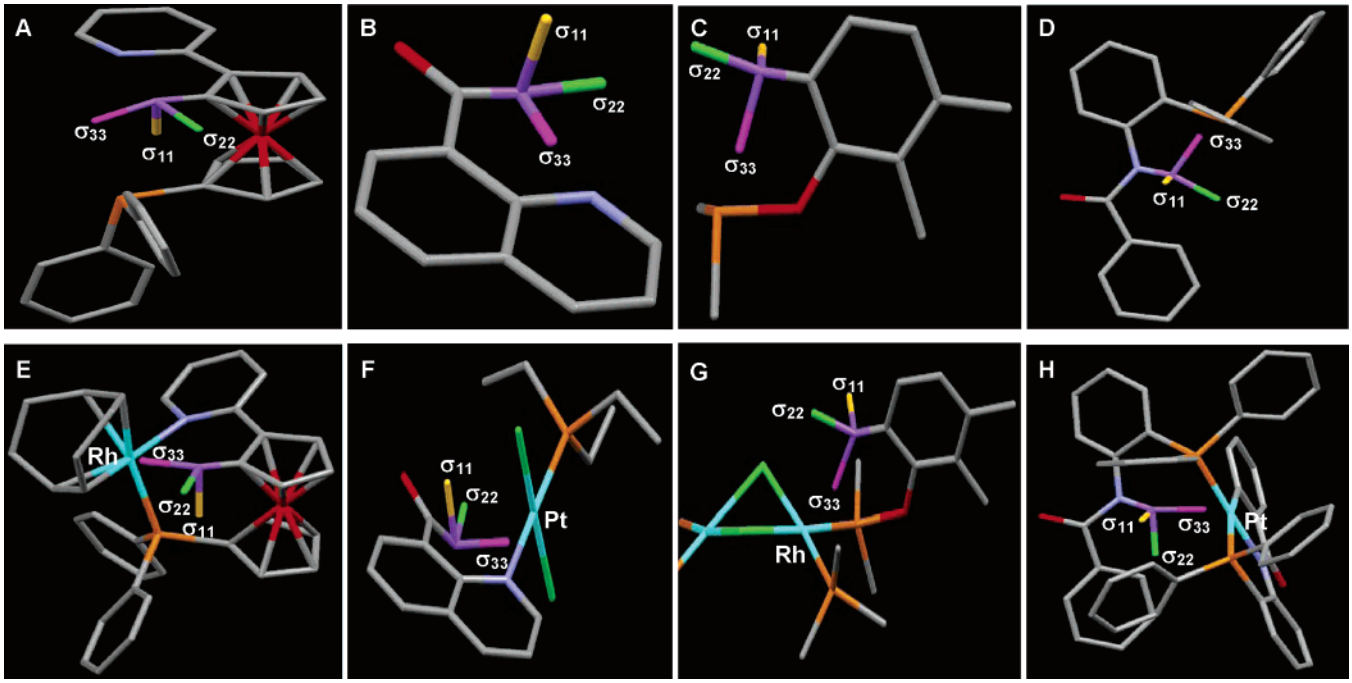

Figure 3. Computed ^{1}H NMR chemical shielding tensor orientations in free ligands (upper panel, A−D) and complexes (lower panel, E−H) of **1**−**4**. The protons and metals of interest and the σ_{11}, σ_{22}, and σ_{33} tensor orientations are in purple, cyan, yellow, green, and pink, respectively. Other protons are omitted for clarity.

Table 2. Computed ^{1}H NMR Isotropic Chemical Shieldings (σ_{iso}) and Chemical Shielding Tensor Elements (ppm)

		σ_{iso}	σ_{11}	σ_{22}	σ_{33}	$\sigma_{33}-\sigma_{11}$
1	complex	23.12	17.37	20.66	31.33	13.96
	ligand	25.95	22.32	27.39	28.13	5.81
2	complex	17.67	11.89	14.65	26.46	14.57
	ligand	19.25	14.22	19.58	23.95	9.73
3	complex	21.67	15.70	20.53	28.77	13.07
	ligand	24.25	19.55	22.83	30.37	10.82
4	complex	19.34	7.01	18.41	32.61	25.60
	ligand	21.22	10.33	22.83	30.51	20.18

Figure 3, each of the ^{1}H NMR shielding tensors rotates on metal bonding, with σ_{33} directed toward the metal centers in the complexes. There are, however, only small changes in the actual magnitudes of σ_{33} between free and metal-bound ligands, while there are more pronounced changes in σ_{11} and σ_{22}, consistent with a large polarization effect along the M···H bond vector (σ_{33}) and the concomitant response of σ_{11} and σ_{22}, perpendicular to this axis. It is also interesting to note in both Rh···H−X complexes (**1**, **3**) and both Pt···H−X complexes (**2**, **4**) that the downfield ^{1}H NMR chemical shift change ($\Delta\delta$) increases with shorter $d_{M\cdots H}$, in both the experimental and the calculated results. For instance, the calculated $\Delta\delta$ in Rh complex **1** with the shorter $d_{M\cdots H}$ (2.35 Å) is 2.83 ppm, which is larger than that of Rh complex **3**, 2.23 ppm, with the longer $d_{M\cdots H}$ (2.80 Å). These isotropic NMR shift results give considerable confidence in the quality of the calculations, which then encouraged us to investigate the somewhat controversial nature of M···H−C interaction (II), using the computed wave functions.

In earlier work, it was proposed that the preagostic interaction (II) involved the metal d_{z^2} orbital.[3,5] For preagostic complex **1**, the HOMO contains the Rh d_{z^2} orbital (Figure 4A); however, this orbital has a different phase from the orbital having the preagostic proton. The first MO involved in the M···H interaction is the HOMO−3 (Figure 4B), having a clear overlap between a Rh $d_{xz/yz}$ and the C−H σ^* orbital. This kind of bonding picture is also apparent in preagostic complex **2**, Figure 4C, where the HOMO has a clear overlap between a Pt $d_{xz/yz}$ and the C−H σ^* orbital. Likewise in preagostic complex **3**, we found no clear evidence for d_{z^2} interaction, with several Rh $d_{xz/yz}$ orbitals being involved. Clearly then, these ab initio calculations of preagostic complexes with various M···H−C interactions indicate that preagostic interactions do not necessarily involve metal d_{z^2} orbitals, as can be seen in Figures 4A−C.

Next, we investigated this topic in more detail using AIM theory[4,22,23] in order to deduce the nature of the M···H−X interactions in these d^8 square planar complexes: are they purely electrostatic (with just penetration of van der Waals radii) or is covalence or partial covalence involved? Here, it is worth briefly reviewing some concepts and nomenclature since using terms such as covalence or partial covalence does rely on their exact definition. In AIM theory, every chemical bond has a bond critical point (BCP) at which the first derivative of the charge density, $\rho(\mathbf{r})$, is zero.[14] The BCP $\rho(\mathbf{r})$ topology is described by a real, symmetric, second-rank Hessian-of-$\rho(\mathbf{r})$ tensor, and the tensor trace is related to the bond interaction energy by a local expression of the virial theorem:[14]

$$\mathrm{Tr(Hessian)} = \nabla^2\rho(\mathbf{r}) = [2G(\mathbf{r}) + V(\mathbf{r})]\,(4m/\hbar^2) \quad (1)$$

where $\nabla^2\rho(\mathbf{r})$ is the Laplacian of $\rho(\mathbf{r})$, and $G(\mathbf{r})$ and $V(\mathbf{r})$ are electronic kinetic and electronic potential energy densities, respectively. Negative and positive $\nabla^2\rho(\mathbf{r})$ values are associated with shared-electron (covalent) interactions and closed-shell

(22) (a) Suresh, C. H.; Koga, N.; Gadre, S. R. *Organometallics* **2000**, *19*, 3008. (b) Uhl, W.; Breher, F. *Organometallics* **2000**, *19*, 4536. (c) Bühl, M.; Håkansson, M.; Mahmoudkhani, A. H.; Öhrström, L. *Organometallics* **2000**, *19*, 5589. (d) Carbó, J. J.; Crochet, P.; Esteruelas, M. A.; Jean, Y.; Lledós, A.; Oñate, E. *Organometallics* **2002**, *21*, 305. (e) Sidorkin, V. F.; Belogolova, E. F.; Pestunovich, V. A. *Organometallics* **2004**, *23*, 2389. (f) Vrček, V.; Bühl, M. *Organometallics* **2006**, *25*, 358.

(23) (a) Carbó, J. J.; Bo, C.; Poblet, J. M.; Moretó, J. M. *Organometallics* **2000**, *19*, 3516. (b) Xu, F.-B.; Li, Q.-S.; Wu, L.-Z.; Leng, X.-B.; Li, Z.-C.; Zeng, X.-S.; Chow, Y. L.; Zhang, Z.-Z. *Organometallics* **2003**, *22*, 633. (c) Feliz, M.; Freixa, Z.; van Leeuwen, P. W. N. M.; Bo, C. *Organometallics* **2005**, *24*, 5718.

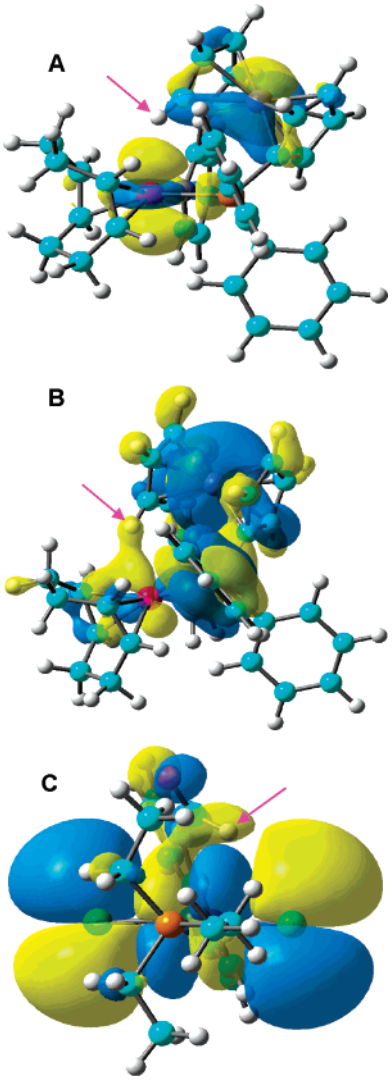

Figure 4. (A) HOMO in **1** (contour value = ±0.03 au). (B) HOMO−3 in **1** (contour value = ±0.015 au). (C) HOMO in **2** (contour value = ±0.005 au). Protons involved in the preagostic interactions are highlighted by pink arrows.

(electrostatic) interactions, respectively.[14] In the latter case, one can further evaluate the total energy density, $H(\mathbf{r})$, at the BCP:

$$H(\mathbf{r}) = G(\mathbf{r}) + V(\mathbf{r}) \qquad (2)$$

A negative $H(\mathbf{r})$ is termed partially covalence, while a positive $H(\mathbf{r})$ indicates a purely closed-shell, electrostatic interaction.[15,24]

It should be noted that, although the absolute values of the BCP properties of complexes **1**−**4** are small (Table 1), as expected they are actually very similar to the results seen in other weak, nonbonded interactions in nonmetal[25] as well as in organometallic compounds.[23] Overall, as shown in Table 1, the BCP properties found in both preagostic (II) and HB (III) complexes are in the same range as those found for other, more conventional HB systems, such as peptide backbones in proteins,[15] all of which also have downfield ^{1}H NMR shifts. These properties are clearly much smaller than those of agostic M···H interactions (I)[4] having upfield ^{1}H NMR chemical shifts, Table 1. The BCP Laplacians in all three preagostic complexes (II) and the metal HB complex (III) studied here are positive. Formally, this indicates a closed-shell (noncovalent) electrostatic interaction. Generally, in **1**−**4**, $\rho(\mathbf{r})$, $G(\mathbf{r})$ and $-V(\mathbf{r})$ decrease with increasing $d_{M\cdots H}$, Table 1, as would be expected for an electrostatic interaction. However, as noted previously,[15,26] use of both $\nabla^2\rho(\mathbf{r})$ and $H(\mathbf{r})$ together enables a more quantitative classification of these HB types: (1) purely electrostatic, weak HB, with $\nabla^2\rho(\mathbf{r}) > 0$ and $H(\mathbf{r}) > 0$; (2) partially covalent, medium HB, with $\nabla^2\rho(\mathbf{r}) > 0$ and $H(\mathbf{r}) < 0$; and (3) covalent, strong HB, with $\nabla^2\rho(\mathbf{r}) < 0$ and $H(\mathbf{r}) < 0$. In the systems under investigation here, we find that $H(\mathbf{r})$ is negative for **1** and **4** but positive for **2** and **3**. This means (in AIM terminology) that the M···H interactions in **1** and **4** have *partial covalence*, while the M···H interactions in **2** and **3** are *purely electrostatic*. This arises most likely from the fact that both **1** and **4** have very short (2.39, 2.32 Å, experimental; 2.35, 2.37 Å, optimized) M···H bond lengths, Table 1, to be compared with the 2.56 and 3.01 Å (experimental) and 2.51 and 2.80 Å (optimized) values found in **2** and **3**, where $H(\mathbf{r}) > 0$. The observation of a more negative $H(\mathbf{r})$ with decreasing HB distance was also observed in other HB systems[26] and in other nonbonded interactions.[25] Clearly then, all four complexes (both preagostic and hydrogen bond) can be regarded as involving purely closed-shell, electrostatic interactions (similar to those found for strong peptide HBs in proteins), with the onset of partial covalence ($H(\mathbf{r}) < 0$) in those systems containing the shortest M···H distances or strongest M···H interactions. Therefore, the above-mentioned relationship of more downfield ^{1}H NMR chemical shift changes ($\Delta\delta$) on complexation with shorter $d_{M\cdots H}$ (in both the Rh···H−X complexes (**1**, **3**) and the Pt···H−X complexes (**2**, **4**)) is a result of increasing covalence (a more negative $H(\mathbf{r})$) in both sets of metal complexes. This is the same trend as found previously in *nonmetal* weak, medium, and strong HB systems (Figure S2); namely, more downfield proton shifts are associated with more negative $H(\mathbf{r})$ values and stronger hydrogen bonding.[15]

Experimental Section

Geometry Optimization. Due to the large sizes (up to 95 atoms) of the complexes studied, geometry optimization was carried out by using the effective core potential basis SDD.[19a] While SDD lacks polarization functions for the lighter elements, the mPW1PW91/SDD[19] method was found to give the best optimized structures for Pt complexes among numerous DFT functionals, using a number of different effective core potential basis sets (LanL2DZ, CEP-31G, CEP-121G, and SDD).[20] The coordinates of the fully optimized complexes using the mpw1pw91/sdd method are provided in the Supporting Information (Tables S1−S4).

NMR Chemical Shift Calculations. We used the B3LYP functional together with a locally dense basis set scheme to calculate the ^{1}H NMR chemical shielding, basically the same approach we used previously to evaluate the NMR properties of other transition metal complexes.[18] We used three layers for the atoms other than the metal: (1) the protons of interest, together with some neighboring atoms, as well as those directly bonded to the metal, were described by a 6-311++G(2d,2p) basis; (2) those atoms bonded to the first-layer atoms were described by a 6-31G* basis; (3) all remaining atoms were described by a 3-21G* basis. For the metals, an SDD basis was used.[19,20] More specifically, the first-layer atoms in complex **1** included the four hydrogen atoms and five carbon atoms in the cyclopentadienyl ring which has the hydrogen of interest, the four carbon atoms directly bonded to Rh, and the P and N atoms directly bonded to Rh. The first-layer atoms in complex **2** included the aldehyde group (CHO) and the carbon atom

(24) Jenkins, S.; Morrison, I. *Chem. Phys. Lett.* **2000**, *317*, 97.
(25) Iwaoka, M.; Komatsu, H.; Katsuda, T.; Tomoda, S. *J. Am. Chem. Soc.* **2004**, *126*, 5309.
(26) Rozas, I.; Alkorta, I.; Elguero, J. *J. Am. Chem. Soc.* **2000**, *122*, 11154.

directly bonded to this aldehyde carbon, plus the two chlorine atoms and the P and N atoms directly bonded to Pt. In the shift calculation of the dimeric complex (**3**), which has a symmetric ligand set, half of the ligand set was modeled by PH_3 (for PMe_3) and PH_2OH (for Me_2POXy), with the results being reported only for the unmodified ligand fragment. In this case, the first-layer atoms included all the atoms directly bonded to Rh, the O bonded to P, and all carbons together with the *o*-, *m*-, and *p*-protons in the Xy group. The first-layer atoms in complex **4** included the hydrogen-bonded NH group and the two carbon atoms directly bonded to this N atom, as well as the 2 P, 1 C, and 1 N atom, directly bonded to Pt.

Acknowledgment. This work was supported in part by the United States Public Health Service (NIH grant GM-50694).

Supporting Information Available: Coordinates (Tables S1−S4) and more NMR shielding/shift results (Figures S1, S2) are available free of charge via the Internet at http://pubs.acs.org.

OM060163H